NASA TECHNICAL NOTE

NASA TN D-5745

c. 1

NASA TN D-5745

DUAL-RATE FINITE-SETTLING-TIME DISCRETE SYSTEMS

by J. A. Gatlin

Goddard Space Flight Center
Greenbelt, Md. 20771

NATIONAL AERONAUTICS AND SPACE ADMINISTRATION • WASHINGTON, D. C. • APRIL 1970

1. Report No.	2. Government Accession No.	3. Recipient's Catalog No.
NASA TN D-5745		
4. Title and Subtitle: DUAL-RATE FINITE-SETTLING-TIME DISCRETE SYSTEMS		5. Report Date: April 1970
		6. Performing Organization Code
7. Author(s): J. A. Gatlin		8. Performing Organization Report No.: G-973
9. Performing Organization Name and Address: NASA Goddard Space Flight Center, Greenbelt, Maryland 20771		10. Work Unit No.: 630-22-01-51
		11. Contract or Grant No.
		13. Type of Report and Period Covered: Technical Note
12. Sponsoring Agency Name and Address: National Aeronautics and Space Administration, Washington, D. C. 20546		14. Sponsoring Agency Code
15. Supplementary Notes		

16. Abstract

Finite settling time response for single input/single output feedback control systems can be obtained using the presented dual-rate, sampled-data control algorithm. The control level is updated every T seconds by the algorithm, which serially accumulates n weighted, plant output error samples during each T second interval. Memory of the previous control level is used to reduce the noise factor of the discrete algorithm. Design examples using amplitude and pulse-width modulation illustrate the design technique. Results of a hybrid computer simulation of the amplitude modulation design present the characteristic transient and steady-state performance obtained.

17. Key Words Suggested by Author	18. Distribution Statement
Sampled-data Discrete systems	Unclassified-Unlimited

19. Security Classif. (of this report)	20. Security Classif. (of this page)	21. No. of Pages	22. Price*
Unclassified	Unclassified	22	$3.00

*For sale by the Clearinghouse for Federal Scientific and Technical Information
Springfie . Virginia 22151

CONTENTS

DUAL-RATE FINITE-SETTLING-TIME DISCRETE SYSTEMS

by
J. A. Gatlin
Goddard Space Flight Center

INTRODUCTION

Finite-settling-time (FST) response for a single output/single input linear feedback control system can be obtained using the dual-rate, sampled-data algorithm

$$-u_{k+1} = b_0(k)\, u_k + \sum_{i=1}^{n} b_i(k)\, \theta_i(k) \; ; \tag{1}$$

u_k = control level, $kT \leq t < (k+1)T$,

$\theta_i(k)$ = output error sampled at $t = (k + i/n)T$,

$b_0(k), b_i(k)$ = controller coefficients, $i = 1, 2, \cdots, n$; $k = 0, 1, 2, \cdots$.

The performance thereby obtained is superior to that obtained using the FST control law for discrete systems discussed by Kalman and Bertram (Reference 1) and Lindorff (Reference 2). Their procedure is based upon the availability of all the state variables and a plant with a rational transfer function, and the design obtained suffers from high noise sensitivity and restricted dynamic range due to plant saturation.

The control law serially accumulates n weighted, plant output error samples, $\theta_i(k)$, $i = 1, \cdots, n$, during each T second interval. Each sample is separated by T/n seconds, with the first sample taken at $t = kT + (T/n)$. At the end of the k^{th} interval, that is, at $t = (k+1)T$, the construction of a new control level is completed. Then, retaining only the value of the previous control level, $b_0(k)\, u_k$, the control law construction cycle repeats.

The synthesis method involves selecting the coefficients $b_i(k)$, $i = 1, \cdots, n$, such that the system is brought to a stable null equilibrium in $m + 1$ control level updates, where m is the order of the plant. Also, the synthesis method minimizes

$$F = \sum_{i=1}^{n} (b_i)^2 \tag{2}$$

in order to minimize input noise transmission.

FORMULATION OF THE PROBLEM

The differential equation describing the plant response for the system shown in Figure 1 can be written as

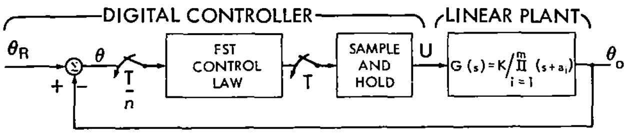

Figure 1—A dual-rate sampled data system.

$$\dot{\mathbf{x}}(t) = \mathbf{G}\mathbf{x}(t) + \mathbf{g}u(t) ,$$

$$u(t) = u_k , \qquad kT \leq t < (k+1)T ,$$

$$\mathbf{x}(0) = \mathbf{x}_0 ; \tag{3}$$

where $\mathbf{G}$ is a $m \times m$ matrix, $\mathbf{x}(t)$ is the plant m-state vector, $\mathbf{x}_0$ defines the plant initial state, and $\mathbf{g}$ is the driving vector which for this single input $u(t)$ has all elements zero except the last which is the control gain constant K. Equation 3 has the solution

$$\mathbf{x}(t) = \Phi(t)\,\mathbf{x}_0 + \Phi(t)\int_0^t \Phi(-\tau)\,\mathbf{g}u(\tau)\,d\tau , \tag{4}$$

where $\Phi(t) = e^{\mathbf{G}t}$ is the plant transition matrix. Letting $\mathbf{x}_k(\ell) = \mathbf{x}(t)|_{t=kT+\ell T/n}$, Equation 3 yields the state vector at the error sample times during the k^{th} interval as

$$\mathbf{x}_k(\ell) = \Phi\left(\frac{\ell T}{n}\right)\mathbf{x}_k(0) + \Phi\left(\frac{\ell T}{n}\right)\int_0^{\ell T/n} \Phi(-\tau)\,\mathbf{g}u(\tau)\,d\tau . \tag{5}$$

Selecting the first element of $\mathbf{x}(t)$ as the plant output variable θ yields the output samples

$$\theta_k(\ell) = \phi_1^T\left(\frac{\ell T}{n}\right)\mathbf{x}_k(0) + \phi_1^T\left(\frac{\ell T}{n}\right)\left[\mathbf{h}\left(\frac{\ell T}{n}\right)\right]u_k , \tag{6}$$

where ϕ_1^T is the first row of the matrix Φ, and

$$\mathbf{h}\left(\frac{\ell T}{n}\right) = \int_0^{\ell T/n} \Phi(-\tau)\,\mathbf{g}\,d\tau . \tag{7}$$

In what follows, $\Phi(\ell T/n)$ will be written as $\Phi(\ell)$. $\phi_1^T(\ell T/n)\,\mathbf{h}(\ell T/n)$, a scalar depending only on ℓ, will be represented by $\alpha(\ell)$. For $\ell = 1, 2, \cdots, n$, Equation 6 produces

$$\begin{bmatrix}\theta_k(1)\\ \vdots \\ \theta_k(n)\end{bmatrix} = \begin{bmatrix}\phi_1^T(1)\\ \vdots \\ \phi_1^T(n)\end{bmatrix}\mathbf{x}_k(0) + \begin{bmatrix}\alpha(1)\\ \vdots \\ \alpha(n)\end{bmatrix}u_k . \tag{8}$$

Defining

$$\mathbf{y}_k^T = \left[\theta_k(1) \cdots \theta_k(n)\right] , \qquad \text{n-vector} ,$$

$$\mathbf{V}^T = \left[\phi_1^T(1) \cdots \phi_1^T(n)\right] , \qquad \text{n} \times \text{m matrix} ,$$

$$\boldsymbol{\alpha}^T = \left[\alpha(1) \cdots \alpha(n)\right] , \qquad \text{n-vector} , \tag{9}$$

reduces Equation 8 to

$$\mathbf{y}_k = \mathbf{V}\,\mathbf{x}_k(0) + \boldsymbol{\alpha}\, u_k . \tag{10}$$

Likewise Equation 1 can be expressed in vector notation as

$$-u_{k+1} = b_0 u_k + \mathbf{b}^T \mathbf{y}_k , \tag{11}$$

where $\mathbf{b}^T = \left[b_1(k) \cdots b_n(k)\right]$. Combining Equations 10 and 11 yields

$$-u_{k+1} = \mathbf{b}^T \mathbf{V}\,\mathbf{x}_k(0) + \left(b_0 + \mathbf{b}^T \boldsymbol{\alpha}\right) u_k . \tag{12}$$

In Equation 12 the output samples, $\theta_i(k)$, have been replaced by a function of the state of the plant at the beginning of the k^{th} control interval, $\mathbf{x}_k(0)$, and control level, u_k, applied during the interval. Let $\mathbf{c}$, an m-vector, be defined as

$$\mathbf{c}^T = \mathbf{b}^T \mathbf{V} ,$$

$$\mathbf{c} = \mathbf{V}^T \mathbf{b} , \tag{13}$$

so that Equation 12 also has the form

$$-u_{k+1} = \mathbf{c}^T \mathbf{x}_k(0) + c_0 u_k , \tag{14}$$

where $c_0 = b_0 + \mathbf{b}^T \boldsymbol{\alpha}$.

The control vector $\mathbf{c}^T$, c_0 can be synthesized from the weighting vector b_0, $\mathbf{b}^T$ as follows. For $n = m$

$$\mathbf{b} = \left[\mathbf{V}^T\right]^{-1} \mathbf{c} ,$$

$$b_0 = c_0 - \mathbf{b}^T \boldsymbol{\alpha} , \tag{15}$$

and for $n \geq m + 1$, b_0 can be left as a free parameter so that

$$\mathbf{C}_{m+1} = \begin{bmatrix} \mathbf{c} \\ \hdashline c_0 - b_0 \end{bmatrix} = \begin{bmatrix} \mathbf{V}^T \\ \hdashline \boldsymbol{\alpha}^T \end{bmatrix} \mathbf{b} = \mathbf{H}\mathbf{b} . \tag{16}$$

Thus for $n = m + 1$,

$$\mathbf{b}(b_0) = \mathbf{H}^{-1} \mathbf{C}_{m+1} , \tag{17}$$

and for $n > m + 1$, the solution of Equation 16 that also minimizes

$$F = \sum_{i=1}^{n} b_i^2$$

is

$$\mathbf{b}_{OPT}(b_0) = \mathbf{H}^T \left[\mathbf{H}\mathbf{H}^T\right]^{-1} \mathbf{C}_{m+1} . \tag{18}$$

Also, if b_0 is not left as a free parameter for $n > m$,

$$\mathbf{b}_{OPT} = \mathbf{V}\left[\mathbf{V}^T \mathbf{V}\right]^{-1} \mathbf{c} ,$$

$$(b_0)_{OPT} = c_0 - \mathbf{b}_{OPT}^T \boldsymbol{\alpha} . \tag{19}$$

For either Equation 17 or 18, b_0 may be either arbitrarily selected, or selected so that F is also minimized with respect to b_0.

Minimization of the noise content factor, F, results in minimum noise transmission through the controller since for white noise input,

$$\sigma_u^2 / \sigma_\theta^2 = F , \tag{20}$$

where σ_u^2 is the variance of the control level sequence and σ_θ^2 is the variance of the output sample sequence.

In this section the equivalence between Equations 1 and 14 has been developed. In the following section the unique values of $\mathbf{c}^T$, c_0 required for FST response will be determined. The values of

b_0, $\mathbf{b}^T$ used in Equation 1 are not unique but depend on the number and the format of the error samples. Equations 15, 17, 18, and 19 can be used to determine the values of b_0, $\mathbf{b}^T$ required to construct any given $(m + 1)$ control vector $\mathbf{c}^T$, c_0.

DETERMINATION OF THE FST CONTROL VECTOR

The change in the state of the plant during the k^{th} interval is given by Equation 5 with $\ell = n$:

$$\mathbf{x}_k(n) = \mathbf{x}_{k+1}(0) = \Phi(n)\,\mathbf{x}_k(0) + \Phi(n)\,\mathbf{h}(n)\,u_k \,. \tag{21}$$

Equations 14 and 21 can be combined to yield

$$\begin{bmatrix} \mathbf{x}_{k+1} \\ \hdashline u_{k+1} \end{bmatrix} = \mathbf{A} \begin{bmatrix} \mathbf{x}_k(0) \\ \hdashline u_k \end{bmatrix} , \tag{22}$$

where

$$\mathbf{A} = \left[\begin{array}{c:c} \Phi(n) & \Phi(n)\,\mathbf{h}(n) \\ \hdashline -\mathbf{c}^T & -c_0 \end{array}\right] = \left[a_{ij}\right] . \tag{23}$$

The matrix $\mathbf{A}$ is the controller plus plant, closed-loop, state transition matrix. To obtain FST response in $(m + 1)$ steps for any set of initial conditions, the parameters $\mathbf{c}^T$, c_0 must be chosen so that

$$\mathbf{A}^{m+1} \equiv 0 \,. \tag{24}$$

Direct solution of Equation 24 is quite tedious, but from the Caley-Hamilton theorem, Equation 24 is satisfied if $\mathbf{A}$, a $(m + 1) \times (m + 1)$ matrix, has all its eigenvalues equal to zero. The canonical form of such a matrix has zeros everywhere except the diagonal above the main diagonal which contains unity elements. Equation 24 is satisfied for

$$|z\mathbf{I} - \mathbf{A}| = z^{m+1} + \sum_{i=0}^{m} a_i z^i = 0 , \tag{25}$$

if

$$a_i = 0 , \qquad i = 0, 1, \cdots, m \,. \tag{26}$$

There are $(m + 1)$ equations involved in Equation 26 and $(m + 1)$ controller parameters $\mathbf{c}^T$, c_0. In general, expansion of Equation 25 about the last row of $|z\mathbf{I} - \mathbf{A}|$ followed by the conditions of Equation 26 yields

$$\begin{aligned} \mathbf{Q}\mathbf{c} &= \mathbf{q} \, , \\ c_0 &= \text{Trace}\, \Phi(n) \, . \end{aligned} \tag{27}$$

The matrix $\mathbf{Q}$ and the vector $\mathbf{q}$ are systematically obtained from $\mathbf{A}$ as illustrated below for a third-order matrix:

$$\begin{vmatrix} z - a_{11} & - a_{12} & - \alpha_1 \\ - a_{21} & z - a_{22} & - \alpha_2 \\ c_1 & c_2 & z + c_0 \end{vmatrix} = 0 \, . \tag{28}$$

Expanding about the last row yields

$$\begin{aligned} 0 = {} & \left(\alpha_2 a_{12} - \alpha_1 a_{22} + \alpha_1 z\right) c_1 + \left(\alpha_1 a_{21} - \alpha_2 a_{11} + \alpha_2 z\right) c_2 \\ & + \left(a_{11} a_{22} - a_{12} a_{21} - \left(a_{11} + a_{22}\right) z + z^2\right)\left(z + c_0\right) \, . \end{aligned} \tag{29}$$

Setting $a_2 = 0$ produces $c_0 = a_{11} + a_{22}$, and setting $a_1 = 0$, $a_0 = 0$ yields

$$\begin{aligned} \mathbf{Q} &= \begin{bmatrix} \alpha_1 & \alpha_2 \\ \left(\alpha_2 a_{12} - \alpha_1 a_{22}\right) & \left(\alpha_1 a_{21} - \alpha_2 a_{11}\right) \end{bmatrix} , \\ \mathbf{q} &= \begin{bmatrix} c_0^2 - \left(a_{11} a_{22} - a_{12} a_{21}\right) \\ - \left(a_{11} a_{22} - a_{12} a_{21}\right) c_0 \end{bmatrix} . \end{aligned} \tag{30}$$

A SECOND-ORDER SYSTEM WITH REAL ROOTS

Consider the system of Figure 1 with $m = 2$, $a_1 = 0$, and $a_2 = a$. Given the parameters K, a, T, and $n \geq 2$, the controller parameters b_0, $\mathbf{b}^T$ are to be chosen to yield FST transient response and a minimum noise content factor, F. The fictitious controller parameters $\mathbf{c}^T$, c_0, illustrated in Figure 2, are

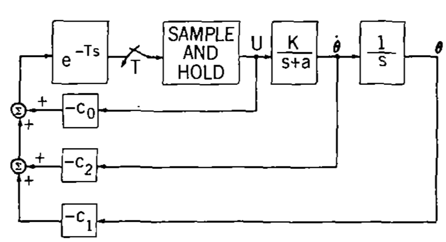

Figure 2—A FST system with direct state variable feedback.

obtained first. Letting $b = e^{-aT}$ results in

$$\Phi(n) = \begin{bmatrix} \phi_{11} & \phi_{12} \\ \phi_{21} & \phi_{22} \end{bmatrix} = \begin{bmatrix} 1 & 1 - b/a \\ 0 & b \end{bmatrix} ,$$

$$\mathbf{h}(n) = \frac{K}{a} \begin{bmatrix} \left(1 + aT - b^{-1}\right)/a \\ \left(b^{-1} - 1\right) \end{bmatrix} , \tag{31}$$

so

$$\Phi(n)\,\mathbf{h}(n) = \frac{K}{a} \begin{bmatrix} (aT + b - 1)/a \\ (1 - b) \end{bmatrix} .$$

As defined in Equation 23, the matrix $\mathbf{A}$ is

$$\mathbf{A} = \left[\begin{array}{cc:c} 1 & \dfrac{(1-b)}{a} & \dfrac{(aT + b - 1)}{(aT)^2} KT^2 \\ 0 & b & \dfrac{(1-b)}{aT} KT \\ \hdashline -c_1 & -c_2 & -c_0 \end{array}\right] ; \tag{32}$$

using Equation 30 yields

$$\begin{bmatrix} c_1 \\ c_2 \end{bmatrix} = \mathbf{Q}^{-1}\mathbf{q} = \begin{bmatrix} \dfrac{aT}{(1-b)KT^2} \\ \dfrac{1 - b - aTb^3}{(1-b)^2 KT} \end{bmatrix} \tag{33}$$

with $c_0 = 1 + b$. It is sometimes useful to set $c_1 = 1$; that is, to use unity static position feedback. This allows the FST loop gain to be expressed as

$$K_0 T^2 = \frac{aT}{(1-b)} , \tag{34}$$

and reduces the expression for c_2 to

$$c_2 = \frac{1 - b - aTb^3}{(1-b)a} . \tag{35}$$

For $n = 2$, Equation 15 yields the weighting parameters b_0, b_1, b_2 from the calculated fictitious controller parameters c_0, c_1, c_2. Using

$$V^T = \begin{bmatrix} 1 & 1 \\ \frac{1-b^{0.5}}{a} & \frac{1-b}{a} \end{bmatrix} , \tag{36}$$

and

$$\alpha = \frac{KT^2}{(aT)^2} \begin{bmatrix} aT/2 + b^{0.5} - 1 \\ aT + b - 1 \end{bmatrix} , \tag{37}$$

consider the case for $aT \sim 0$. Since $e^{-x} = 1 - x + x^2/2! - x^3/3! + \cdots$, the general expressions reduce to

$$K_0 T^2 = aT\Big/\left(aT - \frac{1}{2}(aT)^2 + \cdots\right) \to 1 ,$$

$$c_2 = \frac{1}{a}\left(\frac{aT - \frac{1}{2}(aT)^2 + \cdots - aT + 3(aT)^2 - \cdots}{aT - \frac{1}{2}(aT)^2 + \cdots}\right) \to \frac{5T}{2} , \tag{38}$$

with $c_0 = 2$. Equation 15 now is

$$\mathbf{b} = \begin{bmatrix} 1 & 1 \\ T/2 & T \end{bmatrix}^{-1} \begin{bmatrix} 1 \\ 5T/2 \end{bmatrix} = \begin{bmatrix} -3 \\ 4 \end{bmatrix} ,$$

$$b_0 = 2 - [-3 \quad 4] \begin{bmatrix} 1/8 \\ 1/2 \end{bmatrix} = 3/8 . \tag{39}$$

For $n = 2$ the noise content factor is

$$F = (4)^2 + (3)^2 = 25 . \tag{40}$$

Now consider the use of $n = 3$. The fictitious controller parameters, for $KT^2 = 1$, are

$$C_{m+1} = \begin{bmatrix} c_1 \\ c_2 \\ c_0 - b_0 \end{bmatrix} = \begin{bmatrix} 1 \\ 5T/2 \\ 2 - b_0 \end{bmatrix} , \tag{41}$$

and as defined in Equation 16,

$$\mathbf{H} = \begin{bmatrix} 1 & 1 & 1 \\ T/3 & 2T/3 & 3T/3 \\ 1/18 & 4/18 & 9/18 \end{bmatrix} . \tag{42}$$

Equation 17 yields

$$\begin{aligned} b_1 &= \frac{9}{4} - 9\, b_0 \ , \\ b_2 &= -9 + 18\, b_0 \ , \\ b_3 &= \frac{31}{4} - 9\, b_0 \ . \end{aligned} \tag{43}$$

Calculating the noise content factor and $dF(b_0)/db_0 = 0$ produces

$$(b_0)_{OPT} = -\left(\begin{bmatrix} \frac{9}{4} & -9 & \frac{31}{4} \end{bmatrix} \begin{bmatrix} -9 \\ 18 \\ -9 \end{bmatrix} \right) \Bigg/ \left(\begin{bmatrix} -9 & 18 & -9 \end{bmatrix} \begin{bmatrix} -9 \\ 18 \\ -9 \end{bmatrix} \right) , \tag{44}$$

resulting in $(b_0)_{OPT} = 0.5185$, $F_{MIN} = 15.5$, and

$$\mathbf{b}_{OPT} = \begin{bmatrix} -2.417 \\ 0.333 \\ 3.083 \end{bmatrix} . \tag{45}$$

A unique feature of the general control law expressed by Equation 1 is the incorporation of memory of the previous control level. If $b_0 = 0$ is used, FST response is obtained at the expense of $F = 146$. The low noise transmission feature of the disclosed FST control law is one of its most attractive features.

For $n > m + 1$ the matrix $\mathbf{H}$ is $(m + 1) \times n$. Equation 18 yields, for $n = 4$,

$$\mathbf{b}_{OPT} = \frac{1}{4} \begin{bmatrix} 11 - 32\, b_0 \\ -21 + 32\, b_0 \\ -15 + 32\, b_0 \\ 29 - 32\, b_0 \end{bmatrix} = \begin{bmatrix} -2 \\ -0.5 \\ 1 \\ 2.5 \end{bmatrix} , \tag{46}$$

with $(b_0)_{OPT} = 0.5938$ and $F_{MIN} = 11.5$.

For $n > m + 1$ it is sometimes impractical to use n distinct coefficients. Using only four, Equation 1 takes the form

$$- u_{k+1} = b_0 u_k + b_1 \sum_{i=1}^{n/4} \theta_i (k) + b_2 \sum_{i=n/4+1}^{n/2} \theta_i (k) + b_3 \sum_{i=n/2+1}^{3n/4} \theta_i (k) + b_4 \sum_{i=3n/4+1}^{n} \theta_i (k) . \tag{47}$$

With the error samples thus grouped in 4 sets of $n/4$ samples, the matrix $\mathbf{H}$ is

$$\mathbf{H} = \begin{bmatrix} \frac{n}{4} & \frac{n}{4} & \frac{n}{4} & \frac{n}{4} \\ \frac{n+4}{32} T & \frac{3n+4}{32} T & \frac{5n+4}{32} T & \frac{7n+4}{32} T \\ \frac{n^2+6n+8}{384n} & \frac{7n^2+18n+8}{384n} & \frac{19n^2+30n+8}{384n} & \frac{37n^2+42n+8}{384n} \end{bmatrix} , \tag{48}$$

and for large n, $\mathbf{H}$ becomes

$$\mathbf{H} = \left(\frac{n}{4}\right) \begin{bmatrix} 1 & 1 & 1 & 1 \\ T/8 & 3T/8 & 5T/8 & 7T/8 \\ 1/96 & 7/96 & 19/96 & 37/96 \end{bmatrix} , \tag{49}$$

resulting in

$$\left(\frac{n}{4}\right) \mathbf{b}_{OPT} = \begin{bmatrix} -2.150 \\ -0.550 \\ 1.050 \\ 2.650 \end{bmatrix} , \tag{50}$$

with $(b_0)_{OPT} = 0.8333$ and $F_{MIN} = (13.05)\ (4/n)$.

As $n \to \infty$ Equations 47 and 49 become

$$- u_{k+1} = b_0 u_k + b_1 \int_0^{T/4} \theta(k, t)\, dt + b_2 \int_{T/4}^{T/2} \theta(k, t)\, dt + b_3 \int_{T/2}^{3T/4} \theta(k, t)\, dt + b_4 \int_{3T/4}^{T} \theta(k, t)\, dt ; \tag{51}$$

$$\mathbf{H} = \left(\frac{T}{4}\right) \begin{bmatrix} 1 & 1 & 1 & 1 \\ T/8 & 3T/8 & 5T/8 & 7T/8 \\ 1/96 & 7/96 & 19/96 & 37/96 \end{bmatrix} , \tag{52}$$

with $(T/4)\, b_{OPT} = (n/4)\, b_{OPT}$. The calculation of F_{MIN}, however, must now include the description of the noise source power spectrum. As an example, consider a band-limited noise generator with uniform power density,

$$P_d = \sigma_0^2/f_0 , \qquad -f_0 < f < f_0 , \tag{53}$$

passed through a linear, low-pass filter with the Laplace transfer function

$$G(s) = \frac{\sqrt{\lambda}}{s+\lambda} , \qquad \lambda \ll 2\pi f_0 . \tag{54}$$

The resulting noise source is described by the variance

$$\sigma_e^2 = \frac{1}{j\,2\pi} \int_{-j\infty}^{j\infty} \frac{P_d}{2}\, G(s)\, G(-s)\, ds = \frac{1}{4}\left(\sigma_0^2/f_0\right) , \tag{55}$$

and the auto-correlation function,

$$R_{NN}(\tau) = \sigma_e^2\, e^{-\lambda\tau} . \tag{56}$$

For samples taken every $T/n < 1/\lambda$ seconds, it is no longer appropriate to assume statistical independence of the samples; however, if the noise source is integrated for $T/4 > 1/\lambda$ seconds, samples taken every $T/4$ seconds can be assumed independent with

$$\sigma_I^2 = \int_0^{T/4} \left(\frac{T}{4} - \tau\right) R_{NN}(\tau)\, d\tau , \tag{57}$$

which yields

$$\frac{\sigma_I^2}{\sigma_e^2} = \frac{T}{4\lambda} , \tag{58}$$

$$F = \frac{\sigma_u^2}{\sigma_e^2} = \frac{\sigma_u^2}{\sigma_I^2} \times \frac{\sigma_I^2}{\sigma_e^2} = \left[b_4^2 + b_3^2 + b_2^2 + b_1^2\right] \frac{T}{4\lambda} ,$$

$$F = \left[\left(\frac{T}{4} b_4\right)^2 + \left(\frac{T}{4} b_3\right)^2 + \left(\frac{T}{4} b_2\right)^2 + \left(\frac{T}{4} b_1\right)^2\right] \Big/ \left(\frac{4\lambda}{T}\right)\left(\frac{T}{4}\right)^2 . \tag{59}$$

Therefore, as for Equation 50, $F_{MIN} = (13.05)\,(4/\lambda T)$.

The preceding cases show how F is reduced for $n > m$; Table 1* is given in summary.

Table 1

Effect of Sample Averaging.

n	$(b_0)_{OPT}$	$\sqrt{F_{MIN}}$	$\lambda T/n$
2	0.3750	5.000	1024
3	0.5185	3.937	683
4	0.5938	3.391	512
32	0.8022	1.267	64
128	0.8255	0.637	16
512	0.8314	0.319	4
∞	0.8333	0.160	0

DESIGN EXAMPLES

Consider the system of Figure 1 with $m = 2$, $a_1 = 0$, $a_2 = 0$. The resulting K/s^2 plant model is used as the basic model for many spacecraft single-axis attitude control designs. Using the procedure given in the preceding sections, the matrix $\mathbf{A}$ is

$$\mathbf{A} = \left[\begin{array}{cc|c} 1 & 1 & 0.5\,KT^2 \\ 0 & 1 & KT^2 \\ \hline -1 & -2.5 & -b_0 - (2-b_0)KT^2 \end{array}\right], \qquad \mathbf{x}_k = \begin{bmatrix} \theta \\ T\dot{\theta} \\ u \end{bmatrix}_k \tag{60}$$

with the c^T, c_0 parameters chosen to yield FST response for $KT^2 = 1$. A root locus plot of $\mathbf{A}(KT^2)$, given in Figure 3, illustrates the relative stability of this FST design. Note that for $KT^2 = 0$ there is a z-domain pole at $z = -b_0$; therefore if $b_0 < 1$, system stability for $K_{max} < K < 0$ is obtained.

For $n = 2$ the control algorithm is

$$-u_{k+1} = 4\theta_2(k) - 3\theta_1(k) + (3/8)u_k , \tag{61}$$

*For noise with $R_{NN} = e^{-\lambda\tau}$, $\lambda T = 2048$.

with $F = 25$; for $n = 4$, $F_{min} = 11.5$ for $(b_0)_{OPT} = 0.5938$ and

$$b_{OPT}^T = [-2 \quad -0.5 \quad 1 \quad 2.5] \,. \tag{62}$$

Figure 4 shows how the elements of $\mathbf{b}_{OPT}$ vary for $n = 10$ as a function of b_0, and Figure 5 shows the variation of F with respect to b_0.

If only 3 distinct coefficients, b_2, b_1, b_0, are used with $n = 10$, the control algorithm is

$$-u_{k+1} = (4.4/5)\sum_{i=6}^{10}\theta_i(k) - (3.4/5)\sum_{i=1}^{5}\theta_i(k) + 0.735u_k \,, \tag{63}$$

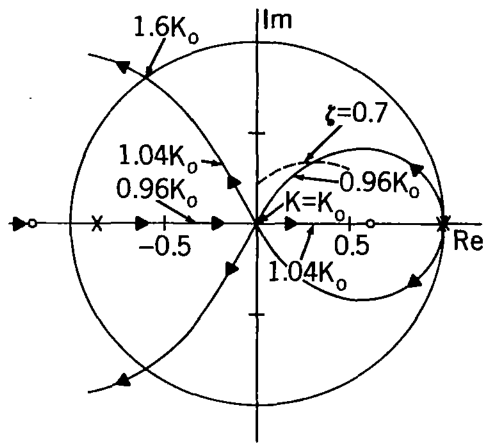

Figure 3—FST root locus for $b_0 = 0.8333$.

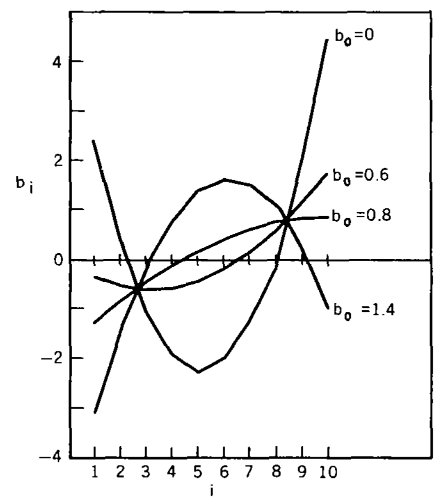

Figure 4—The elements of b_{OPT} for $n = 10$.

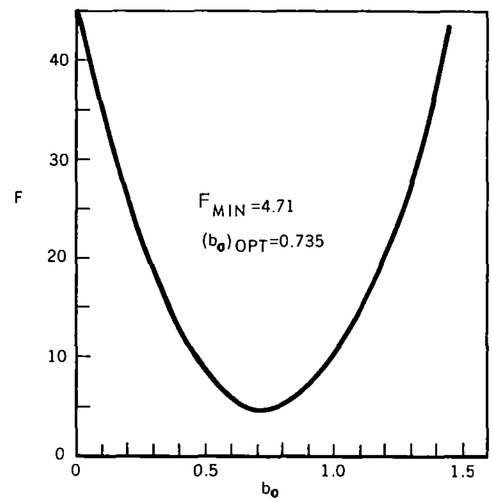

Figure 5—F versus b_0 for $n = 10$.

with $F = \left[(4.4)^2 + (3.4)^2\right]/5 = 6.18$. Thus, for $n = 10$, use of sample averaging to reduce the number of required distinct controller parameters increases the noise factor F by 6.18/4.71 or 31%. For large n, $nb_2/2 = 4.5$, $nb_1/2 = -3.5$, and $F = 85/n$.

Consider now the use of pulse-width-modulation during the T second interval so that reaction jet attitude control torquers can be used. The jet on-time ΔT_k is scaled to apply the same control impulse as the preceding amplitude-modulation design; that is,

$$\Delta T_k \, u_{max} = u_k T \,, \qquad \Delta T_k \leq T \,. \tag{64}$$

The matrix $\mathbf{A}$, now non-linear, becomes

$$\mathbf{A} = \left[\begin{array}{cc|c} 1 & 1 & (1 - 0.5\,\gamma_k)\,KT^2 \\ 0 & 1 & KT^2 \\ \hline -c_1 & -c_2 & -c_0 \end{array}\right], \qquad 0 \le \gamma_k \le 1 , \tag{65}$$

$$\gamma_k = \Delta T_k / T = |u_k| / u_{max} . \tag{66}$$

Applying the linear FST design methods, assuming γ_k is constant, yields finite settling time response as $\gamma_k \to$ constant with $c_0 = 2$, $c_1 = 1$, and $c_2 = 2 + 0.5\,\gamma_k$. Using Equation 19 and 3 distinct controller coefficients yields

$$\left(\frac{n}{2}\right)\mathbf{b} = \begin{bmatrix} -(2.5 + \gamma_k) \\ 3.5 + \gamma_k \end{bmatrix} ,$$

$$b_0 = 2 - \mathbf{b}^T \boldsymbol{\alpha}(\gamma_k) . \tag{67}$$

The elements of $\boldsymbol{\alpha}$ are piecewise continuous functions of γ_k; for example,

$$\boldsymbol{\alpha} = \frac{1}{12}\begin{bmatrix} 3 - 6\gamma_k + 4\gamma_k^2 \\ 9 - 6\gamma_k \end{bmatrix} , \qquad 0 < \gamma_k \le 0.5 . \tag{68}$$

Also for $\gamma_k = 0$, $b_0 = 0$; and for $\gamma_k = 1$, $\mathbf{b}$ and b_0 are the same as used with amplitude modulation.

The matrix $\mathbf{A}$ can be used to examine the non-linear response of this FST design. Defining $\tilde{u}_k$ as the calculated control level and retaining u_k as the control level applied and remembered allows minimum jet on-time and jet full-on conditions to be handled by the logic

$$u_k = 0 , \qquad 0 \le |\tilde{u}_k| \le U_{min}$$

$$u_k = \tilde{u}_k , \qquad U_{min} < |\tilde{u}_k| \le U_{max}$$

$$|u_k| = U_{max} , \qquad U_{max} < |\tilde{u}_k| . \tag{69}$$

For large initial rates the response for $KT^2 = 1$, $U_{max} = 1$, $U_{min} = 0.05$ is given in Tables 2 and 3.

Table 2

Saturated Transient Response.

k	θ_k	$T\dot{\theta}_k$	u_k	$\tilde{u}_k$
0	0	1	0	0
1	1	1	-1	-2
2	1.5	0	-1	-1.5
3	1	-1	0.5	0.5
4	0.375	-0.5	0.25	0.25
5	0.093	-0.25	0.187	0.187
6	0.013	-0.063	0.054	0.054
7	0.004	-0.008	0	0.003
8	-0.004	-0.008	0	0.011
9	-0.012	-0.008	0	0.019
10	-0.02	-0.008	0	0.026

Table 3

Unsaturated Transient Response.

k	θ_k	$T\dot{\theta}_k$	u_k	$\tilde{u}_k$
0	0	0.25	0	0
1	0.25	0.25	-0.5	-0.5
2	0.125	-0.25	0.187	0.187
3	0.044	-0.063	0	0.023
4	-0.018	-0.063	0.08	0.08
5	-0.004	0.017	0	-0.016
6	0.014	0.017	0	-0.032
7	0.031	0.017	0	-0.05
8	0.049	0.017	-0.068	-0.068
9	0.002	-0.05	0	0.048
10	-0.048	-0.05	0.096	0.096

SIMULATION RESULTS

Construction of a FST system to control a second-order plant was accomplished using hybrid simulation. The continuous plant, $G(s) = K/s^2$, was modeled on the analog computer, and digital computation generated the control law of Equation 1 and the output error $\theta = \theta_0 - \theta_R$, where θ_0 is the plant output and θ_R is a staircase reference function that changes every T seconds.

The control law update interval, T, is 11 seconds, of which 10 seconds is used for output sampling and 1 second for the computational and conversion delays; that is, Equation 1 has the form

$$-u_{k+1} = b_0 u_k + b_1 \sum_{i=1}^{n/4} \theta_i(k) + b_2 \sum_{i=n/4+1}^{n/2} \theta_i(k) + b_3 \sum_{i=n/2+1}^{3n/4} \theta_i(k) + b_4 \sum_{i=3n/4+1}^{n} \theta_i(k) + b_5 \sum_{i=n}^{11/\Delta T} \theta_i(k) \tag{70}$$

with $b_5 = 0$ and $n = (T - T_d)/\Delta T = 10/\Delta T$. Output error sampling periods, ΔT, of 10/512, 10/128, and 10/32 seconds are provided; an option allowing the plant output to be integrated for 10/4 seconds on the analog computer and sampled every 10/4 seconds is included.

Since the data sampling interval is now only $(T - T_d)$, Equation 49 becomes

$$\begin{bmatrix} c_1 \\ c_2 \\ c_0 - b_0 \end{bmatrix} = \left(\frac{n}{4}\right) \begin{bmatrix} 1 & 1 & 1 & 1 \\ \frac{(T-T_d)}{8} & \frac{3(T-T_d)}{8} & \frac{5(T-T_d)}{8} & \frac{7(T-T_d)}{8} \\ \frac{(T-T_d)^2/T^2}{96} & \frac{7(T-T_d)^2/T^2}{96} & \frac{19(T-T_d)^2/T^2}{96} & \frac{37(T-T_d)^2/T^2}{96} \end{bmatrix} \begin{bmatrix} b_1 \\ b_2 \\ b_3 \\ b_4 \end{bmatrix}, \quad (71)$$

and letting $d = T_d/(T - T_d)$, Equation 71 reduces to

$$\begin{bmatrix} c_1 \\ (1+d)\, c_2\, T \\ (1+d)^2 (c_0 - b_0) \end{bmatrix} = \left(\frac{n}{4}\right) \begin{bmatrix} 1 & 1 & 1 & 1 \\ 1/8 & 3/8 & 5/8 & 7/8 \\ 1/96 & 7/69 & 19/96 & 37/96 \end{bmatrix} \begin{bmatrix} b_1 \\ b_2 \\ b_3 \\ b_4 \end{bmatrix}. \quad (72)$$

As shown in Reference 3, the relative stability as described by the root locus plot (Figure 3) depends only on the plant gain, K, and the value of b_0. If b_0 is kept at the value of $(b_0)_{OPT}$ for $d = 0$, the addition of the delay affects only the value of F. The inverse of Equation 72 yields

$$\left(\frac{n}{4}\right) \mathbf{b} = \begin{bmatrix} -2.150 \\ -0.550 \\ 1.050 \\ 2.650 \end{bmatrix} + d \begin{bmatrix} 5.667 \\ -9.667 \\ -7.667 \\ 11.667 \end{bmatrix} + \left(\frac{28}{3}\right) d^2 \begin{bmatrix} 1 \\ -1 \\ -1 \\ 1 \end{bmatrix} \quad (73)$$

for $b_0 = 0.8333$. For $d = 1/10$,

$$\left(\frac{n}{4}\right) \mathbf{b} = \begin{bmatrix} -1.490 \\ -1.610 \\ 0.190 \\ 3.910 \end{bmatrix} \quad (74)$$

with $F = (20.13)\,(4/n)$ which corresponds to an increase in F of 54%.

As developed previously (Equations 34 and 38) the FST loop gain requires a plant constant, K_0, such that

$$K_0 = \frac{1}{T^2} = \frac{1}{(11)^2} = \frac{1}{121} \frac{\text{volts}}{\text{sec}^2}.$$

If $K \neq K_0$, a non-finite but rapidly convergent sequence will characterize the transient response. Figure 6 presents this effect for an initial condition response, $\dot{\theta}_0 \neq 0$, $\theta_0 = 0$; Figures 7, 8, 9 show this effect when the controller is tracking an input "staircase" sinusoid.

The coefficient set of Equation 74 is exact for $n \to \infty$ and is a good approximate set for large n. Figure 10 shows the effect of the approximation for $n = 32$, $n = 128$, and $n = 512$; Figure 11 compares the sampling format for finite and infinite n.

The steady-state performance when output noise is present shows, in Figure 12, the reduction of the controller noise sensitivity as the error sampling rate is increased. The runs in Figure 10 correspond to the values of $n = 32$, 128, 512, and ∞ given in Table 1 of the preceding section. Figure 13 presents a transient response with noise present for $n = 512$.

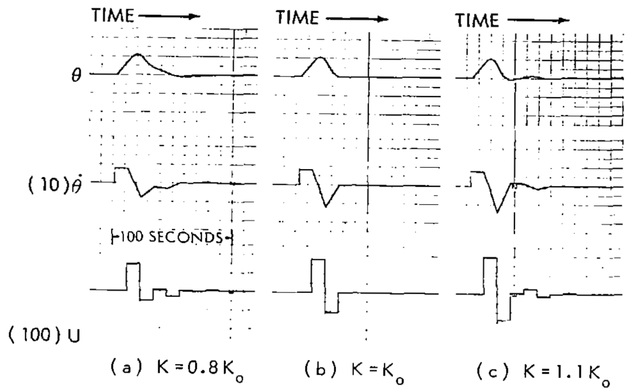

Figure 6—Initial rate transient response.

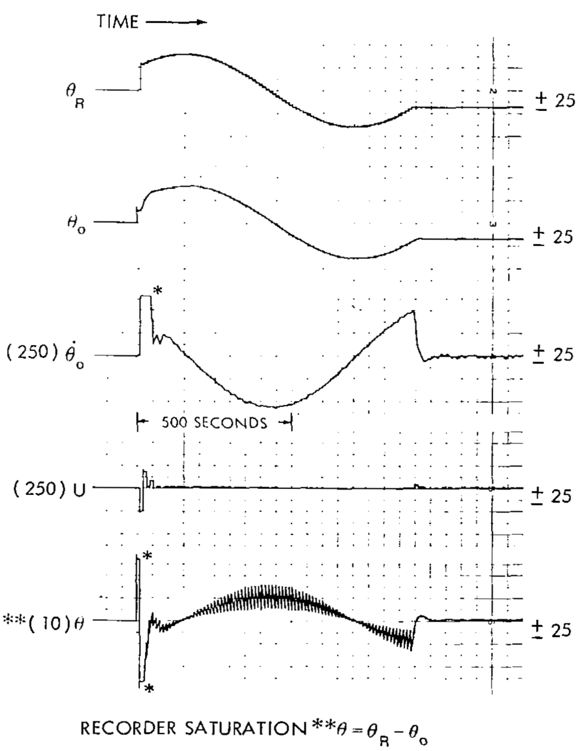

Figure 7—Tracking response for $K = 0.8 K_0$.

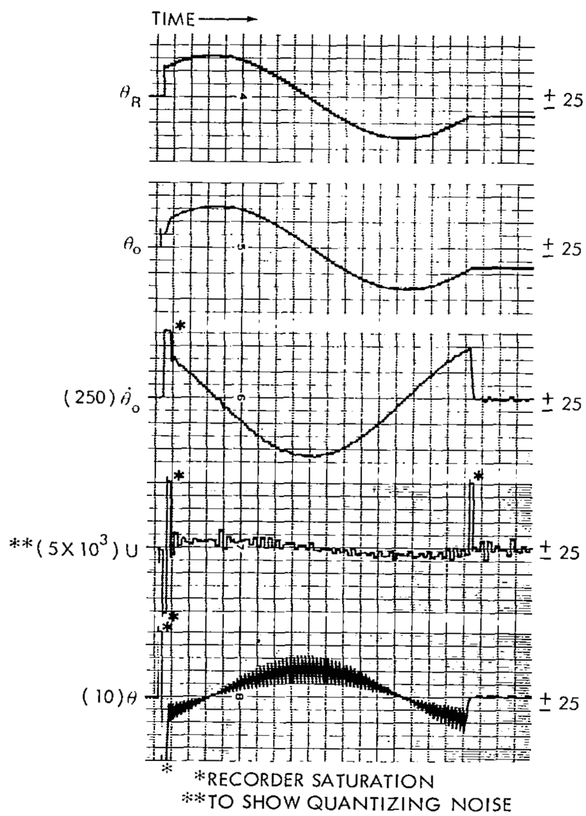

Figure 8—Tracking response for $K = K_0$.

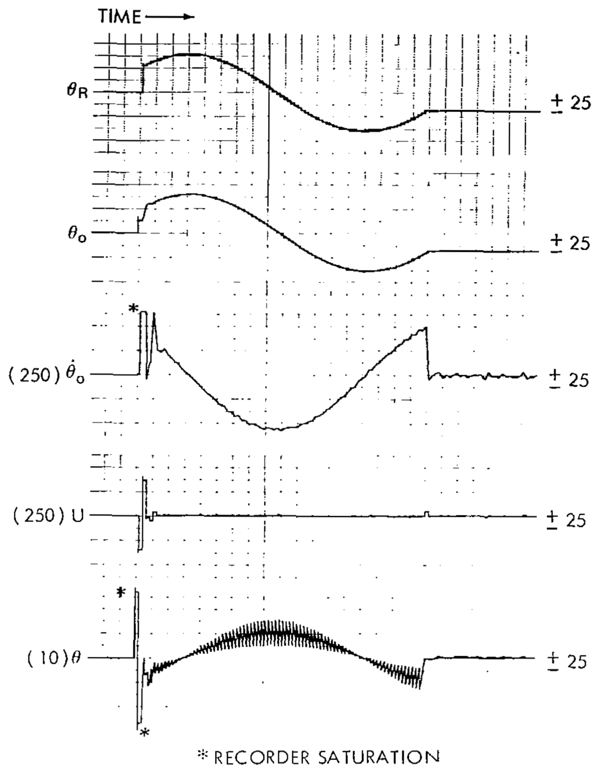

Figure 9—Tracking response for K = 1.1 K_0.

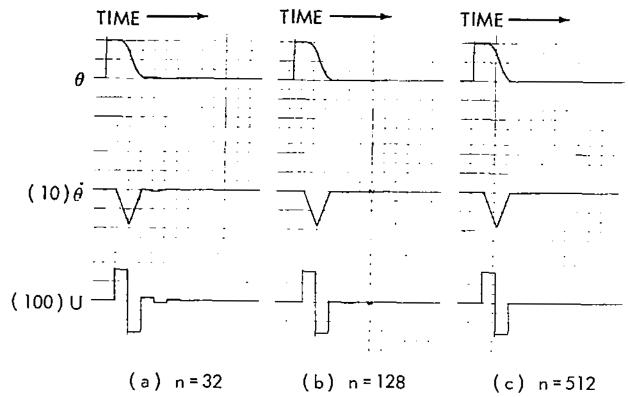

Figure 10—The effect of the large n assumption.

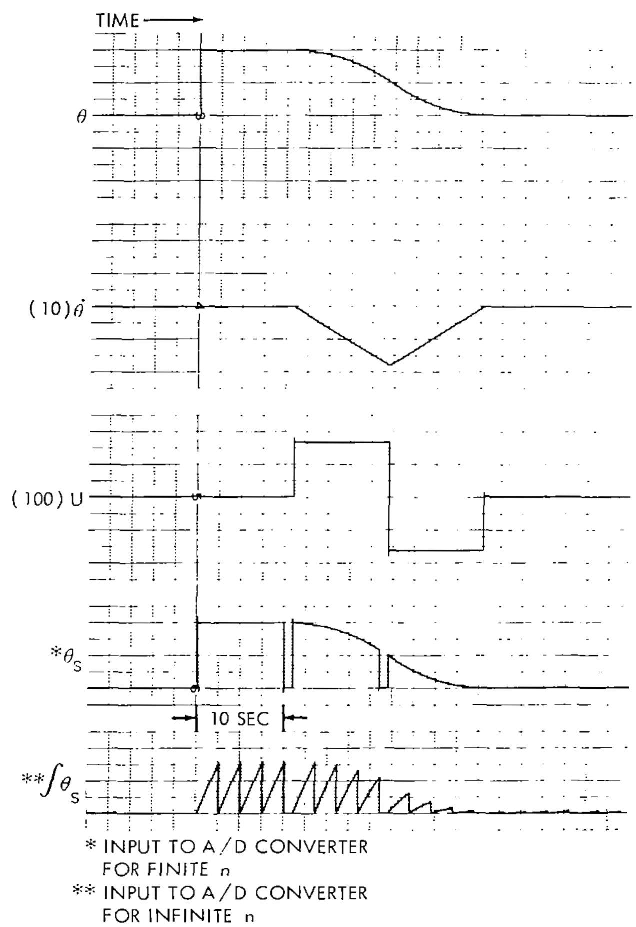

Figure 11—Error sampling format.

CONCLUSIONS

This paper has extended the work done in Reference 3 so that the dual-rate FST control law can be applied to n^{th} order single-input, single-output systems. A means of handling computation and conversion delays, additional noise analysis, and additional hybrid simulation work is also documented.

The general control law formulation given in Equation 1 allows for the controller coefficients $b_0(k)$, $b_i(k)$ to be a function of the control interval index, k. In one of the design examples presented in this report, the coefficients required are constant. The need for varying coefficients arises when the matrix **A** (Equation 23) has elements that change from control interval to control interval. This requires that

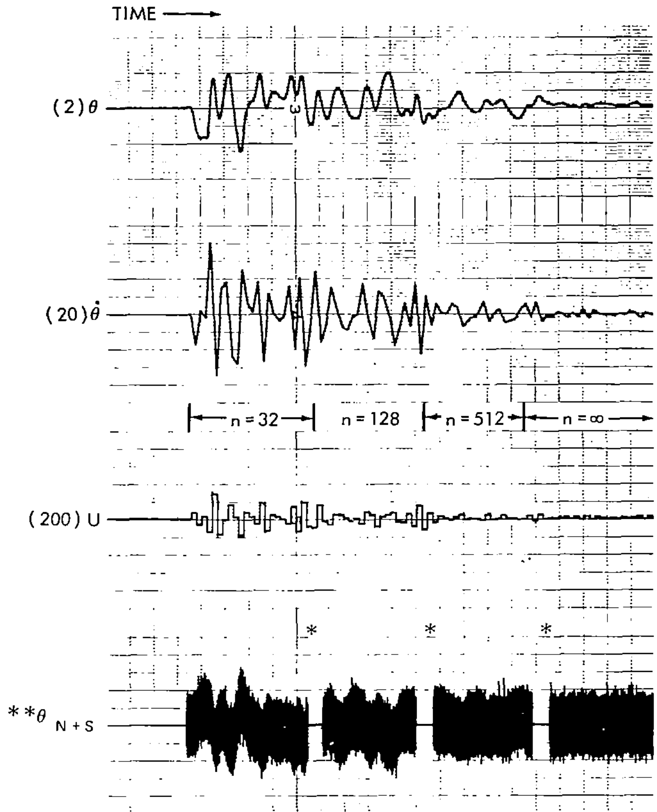

Figure 12—Steady state performance with noise.

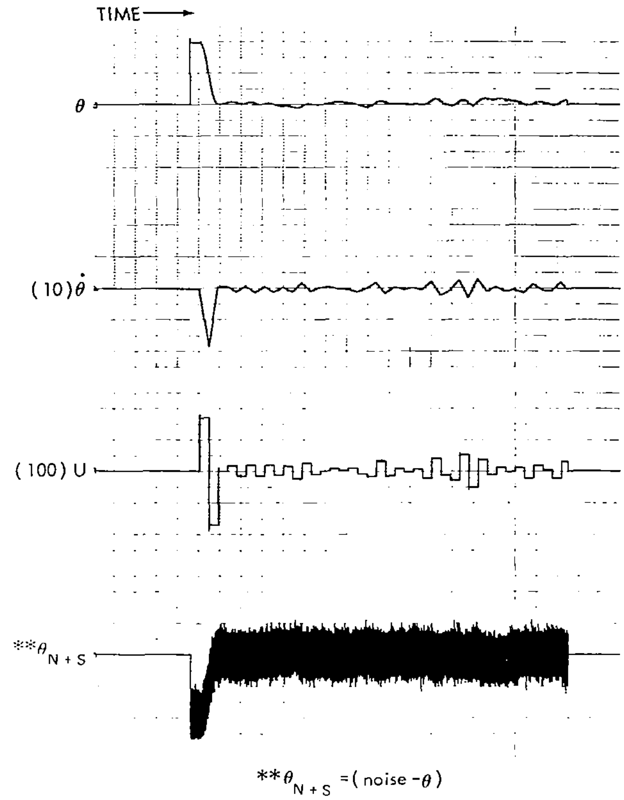

Figure 13—Transient performance with noise.

the control vector c^T, c_0 also be a function of k if A is to approach an FST matrix as its elements approach a constant value. This approach has been used to apply the FST control law to pulse-width-modulation control of a second-order plant. The elements of A can also change due to changes in the equilibrium position of a non-linear plant. Thus, using the non-linear model, the coefficients $b_0(k)$, $b_i(k)$ can be adjusted to "track the operating point" and maintain FST response about the operating point.

In summary the key features of the new FST control law are:

(1) The dual error sampling/control level update rates allow the error sampling rate to be chosen to meet noise sensitivity requirements and the control update rate chosen to avoid plant saturation.

(2) The memory of the previous control level greatly reduces the need for the controller coefficients to produce derived error rate information.

(3) Only the output state need be directly sensed; all the state variables appear combined in the generated control level, but their isolation is not required.

(4) The control technique possesses null stability and reasonable tolerance to errors in the plant model.

(5) The finite memory of the control law allows the controller weighting coefficients to be readily changed during each control interval.

(6) A multiplicity of error samples taken while the control level remains constant provides a source of data for plant and disturbance on-line modeling.

Goddard Space Flight Center
National Aeronautics and Space Administration
Greenbelt, Maryland, December 15, 1969
630-22-01-01-51

REFERENCES

1. Kalman, R. E., and Betram, J. E., "General Procedure for Computer Control of Single-loop and Multiloop Linear Systems," *Trans. AIEE,* 78(2):602-609, 1959.

2. Lindorff, D. P., *Theory of Sampled-data Control Systems,* New York: John Wiley, 1965.

3. Gatlin, J. A., "Development of a Simple Digital Control Law for Spin Phase Synchronization of a Cartwheel Satellite in a Circular Polar Orbit," *Ph.D. Thesis,* University of Maryland, 1968.

NASA-Langley, 1970 —— 10